

FISM-P: Modeling Solar VUV Variability Throughout the Solar System

Thiemann, Edward M.B.¹; Eparvier, Francis G.¹; Chamberlin, Philip C.²

¹Laboratory For Atmospheric and Space Physics, University of Colorado, Boulder, CO, USA; ²Solar Physics Laboratory, NASA Goddard Space Flight Center, Greenbelt, MD, USA

Contact for questions and comments: Thiemann@lasp.colorado.edu

INTRODUCTION

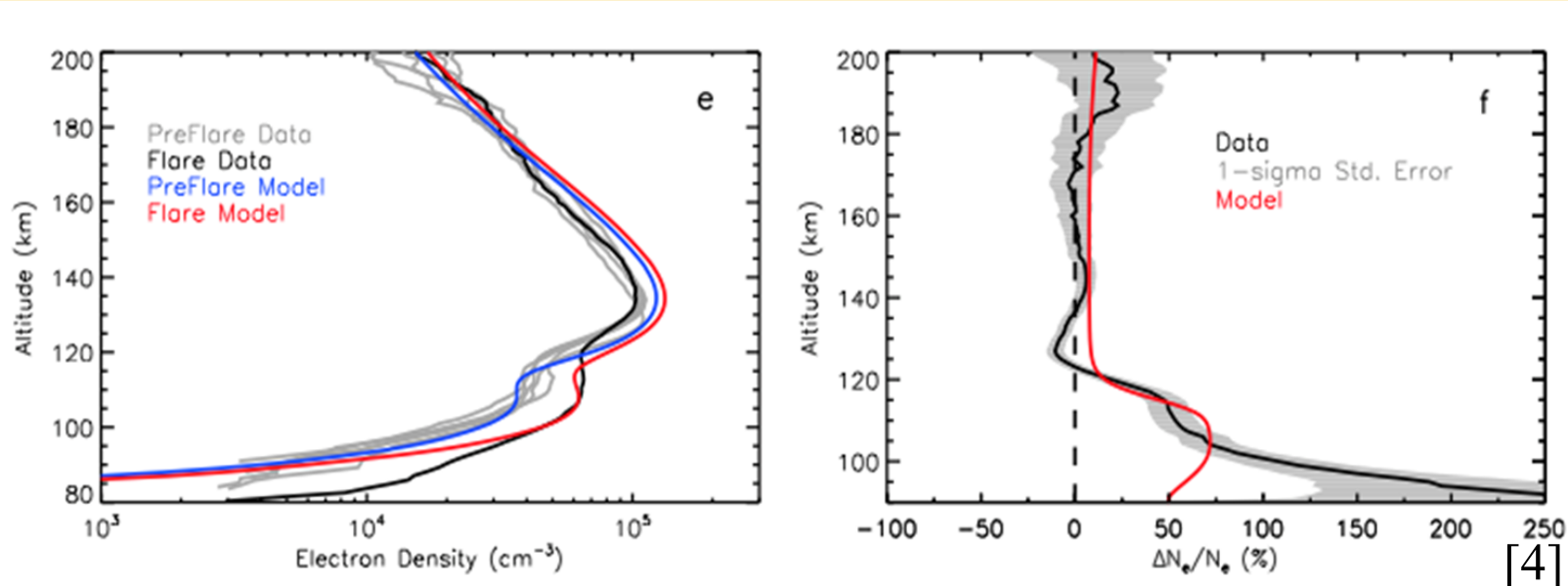
The Flare Irradiance Spectral Model (FISM) is an empirical model of the solar vacuum ultraviolet (VUV: 0-190 nm) irradiance spectrum from .1 to 190 nm at 1 nm spectral resolution with a 1 minute time cadence. This latest iteration, called FISM-Planetary (FISM-P), estimates mean daily irradiances throughout the solar system using weighted interpolation of the best available proxies for each layer of the solar atmosphere (chromosphere, transition region, cool corona, and hot corona). In addition to daily irradiances, planetary 1-minute (flaring) irradiances are available if the flaring emissions are observed by instruments at Earth or MAVEN-EUV at Mars. FISM has been successfully used as an input for ionospheric and thermospheric models for Earth, Mars, and surface charging of the moon, e.g. [3,4,5]. FISM-P now provides the capability for similar studies throughout the solar system and when combined with the MAVEN-EUV channels (H Ly- α , 17-22 nm and 0-6 nm), will provide unprecedented accuracy at Mars.

Key Points:

- FISM-P interpolates irradiances from Earth around the ecliptic based on Carrington rotation.
- FISM-P performs nearly as well with only 3 common proxies as FISM-Earth does with the full suite of 12 proxies.
- FISM-P can use a 0.1-7 nm band flare proxy in lieu of XRS-B to model flares from the vantage point of Mars.
- FISM-P can possibly use far-side magnetograms as a proxy. MAVEN-EUV can test this concept.

BACKGROUND

Solar flares perturb planetary ionospheres from an equilibrium state as is well known from our experience at Earth, and their impact can be studied by comparing models to measurement. Because these models depend on the incident EUV spectral flux, knowing the incident spectrum to a high degree of accuracy can better constrain these models. The figures below show model and measurement results for an X class flare at Mars. The discrepancy at low altitudes suggests a need for improved planetary flare modeling.



The FISM Proxy Model

First developed in 2007, FISM decomposes solar irradiance variability into solar cycle and solar rotation components which are summed with a (constant) minimum spectrum to produce the irradiance for a given wavelength bin. [1,2]. Flaring contributions can be decomposed into gradual phase and impulsive phase contributions.

$$E(\lambda, t) = E_{min}(\lambda) + \Delta E_{SC}(\lambda, t) + \Delta E_{SR}(\lambda, t) + \Delta E_{GP}(\lambda, t) + \Delta E_{IP}(\lambda, t)$$

The solar cycle and rotation variability components are found using 108 day averages of the daily irradiance value:

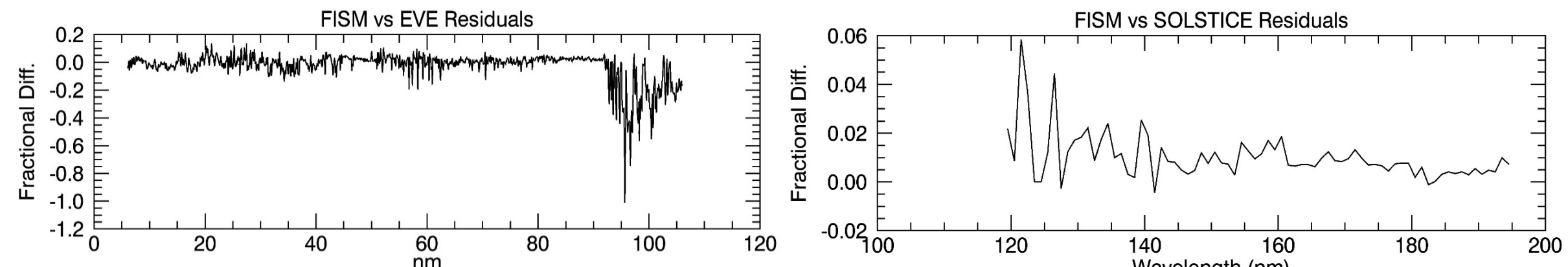
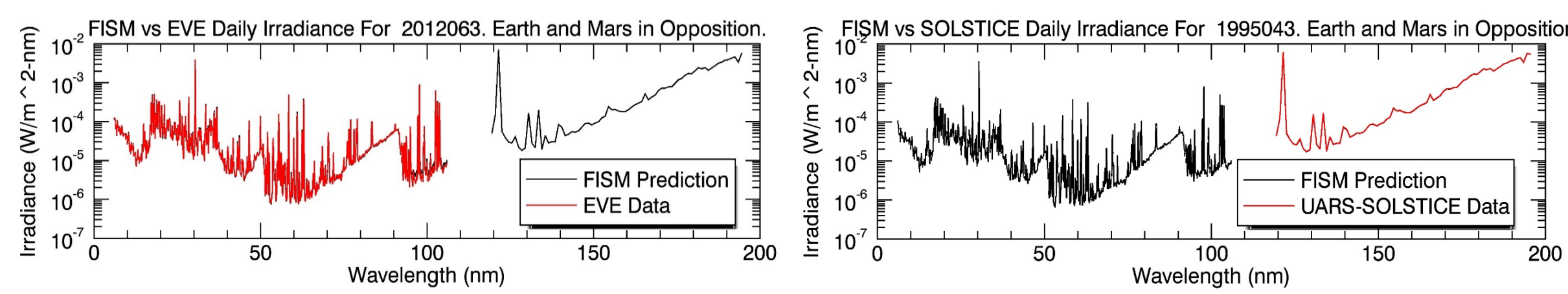
$$\Delta E_{SR}(\lambda, t_d) = E_d(\lambda, t_d) - \langle E_d(\lambda, t_d) \rangle_{108}$$

$$\Delta E_{SC}(\lambda, t_d) = \langle E_d(\lambda, t_d) \rangle_{108} - E(\lambda)_{min}$$

A linear relation is assumed between the proxy and irradiance bin.

$$\frac{\langle E_d(\lambda, t_d) \rangle_{108} - E(\lambda)_{min}}{E(\lambda)_{min}} = C_0(\lambda) + C_{SC}(\lambda) \left[\frac{\langle P_d(t_d) \rangle_{108} - P_{min}}{P_{min}} \right]$$

$$\frac{E_d(\lambda, t_d) - \langle E_d(\lambda, t_d) \rangle_{108}}{E(\lambda)_{min}} = C_1(\lambda) + C_{SR}(\lambda) \left[\frac{P_d(t_d) - \langle P_d(t_d) \rangle_{108}}{P_{min}} \right]$$



PLANETARY INTERPOLATION MODEL

The Driving Proxies

To estimate daily averaged solar VUV irradiance throughout the solar system, FISM-P interpolates the proxies to the Carrington Day (CD) of interest using a weighted average of daily irradiances from the preceding and following solar rotations where the heliographic longitude of interest is disk center with respect to earth. A single CD is defined as 13.2° of solar rotation. These interpolated proxy values constitute the Driving Proxies, and are used to drive the FISM model to estimate the VUV spectral irradiance at the CD of interest.

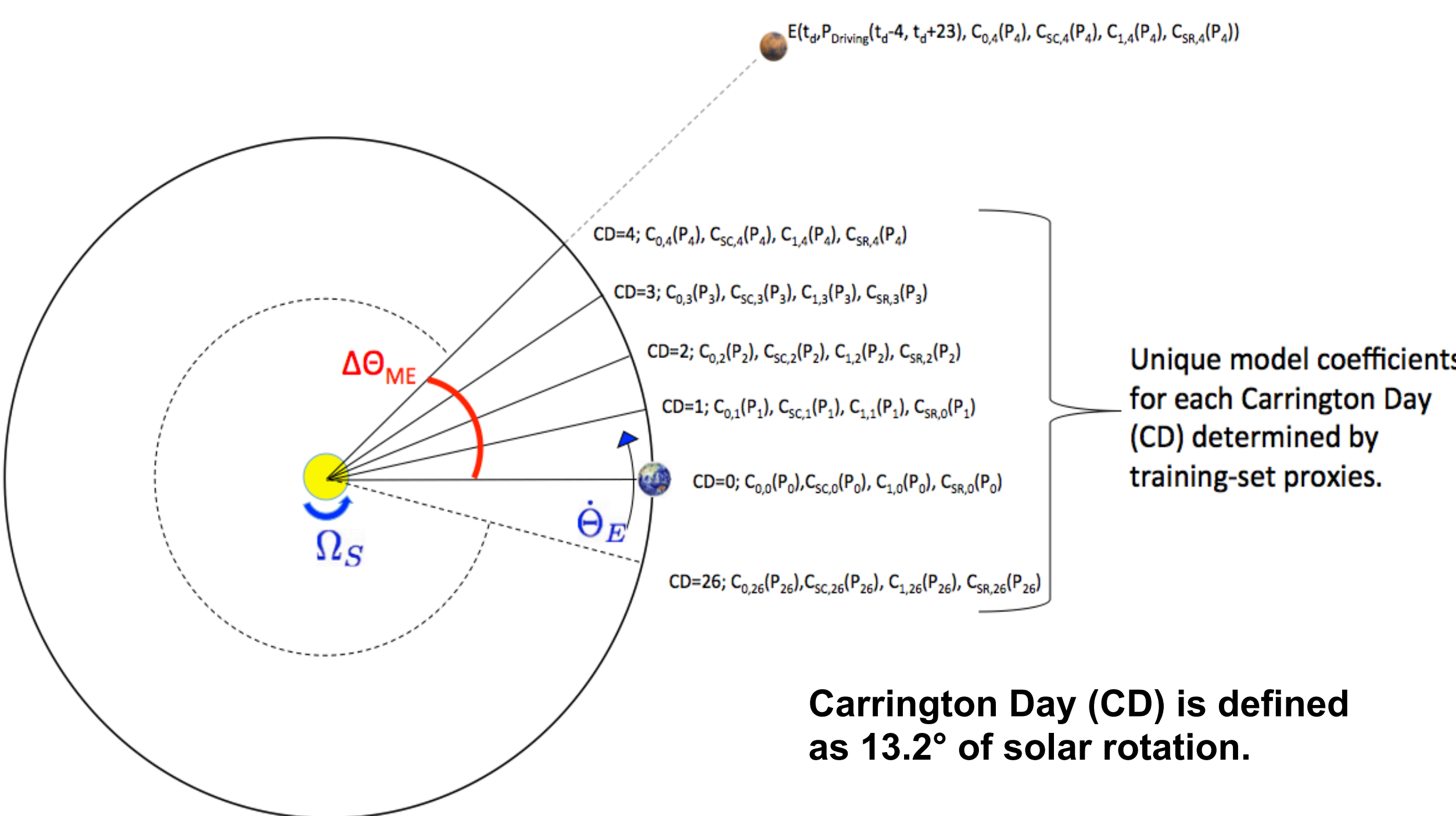
$$P(t_d, \Theta_{planet}) = (w_1 \cdot P(t_d - \Delta t_1) + w_2 \cdot P(t_d + \Delta t_2))$$

$$w_{1,2} = \frac{\Delta t_{1,2}}{\Delta t_1 + \Delta t_2}$$

$$\Delta t_1 = \frac{2\pi - |\Delta\Theta(t_d)_{planet-earth}|}{\Omega_s - \dot{\Theta}_E} \quad \Delta t_2 = \frac{|\Delta\Theta(t_d)_{planet-earth}|}{\Omega_s - \dot{\Theta}_E}$$

The Training Set Proxies

Rather than using a single set of model coefficients for each of the 27 CDs, a set of coefficients is trained for each CD by effectively interpolating the training-set proxies, resulting in a library of 27 sets of coefficients. This is done by taking a weighted average of irradiance measurements for the day of interest, called the Direct Component, with values for that day as determined by linearly interpolating irradiance measurements from the prior and subsequent solar rotations which is called the Interpolated Component. As the CD increases from 0 to 13, the weighting of the Interpolated Component increases and the Direct Component weighting decreases. As the CD increases from 14 to 27, the Direct Component weight increases and the Indirect Component Decreases. It is important to remember that these Training-Set Proxies are irradiances at Earth and have been conditioned to represent measurements from other, non-Earth, positions along the heliographic plane interpolated to Earth; whereas the Driving Proxies represent irradiances at non-Earth positions along the heliographic plane interpolated from Earth.

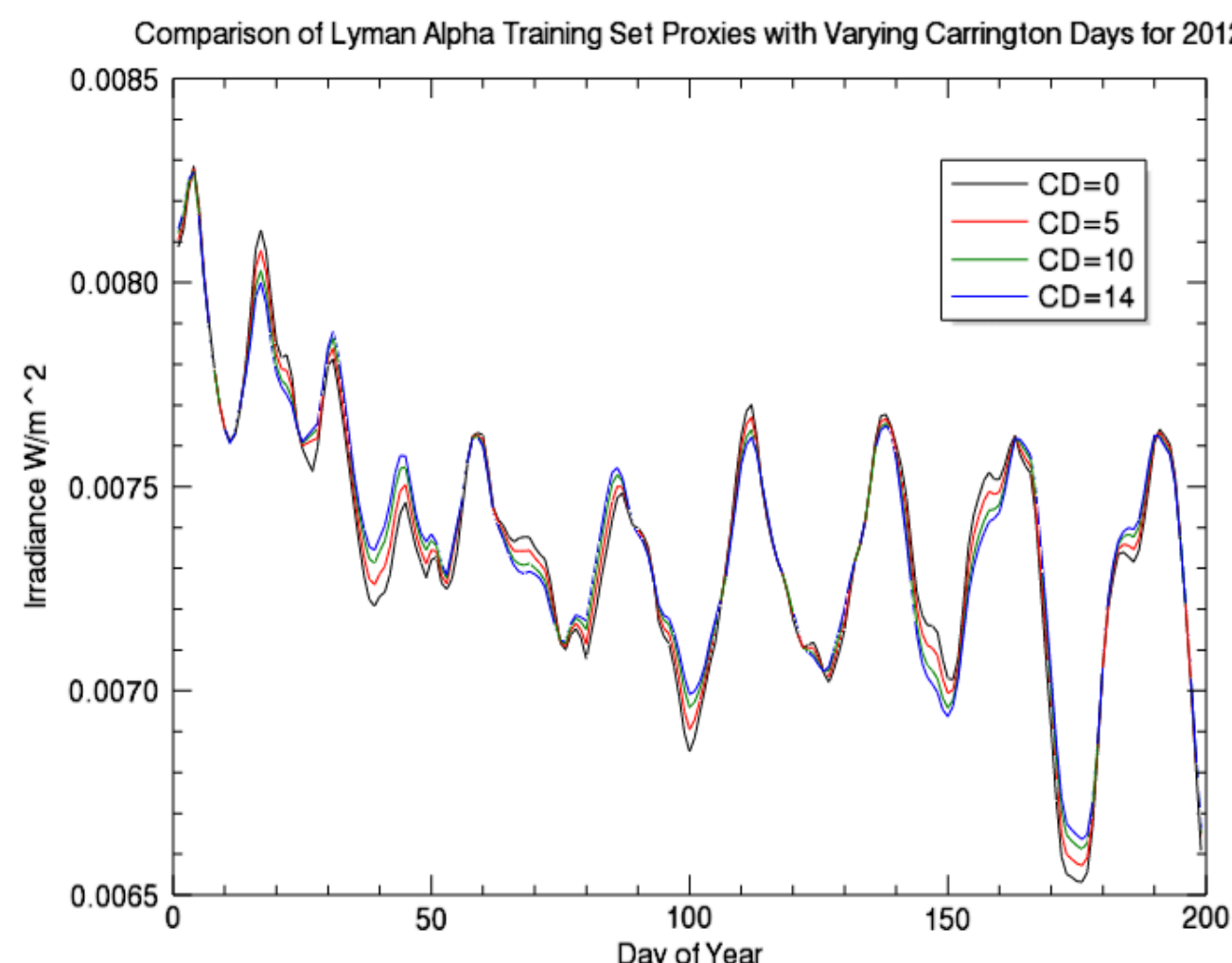


$$P_{SRD} = w_{TS} \cdot P_{DC} + (1 - w_{TS}) \cdot P_{IC}$$

$$w_{TS} = \frac{1}{2} + \frac{1}{2} (1 - \min(\Delta t_1, \Delta t_2) \cdot 2 \cdot (\Omega_s - \dot{\Theta}_E))$$

$$P_{IC}(t_d) = \frac{1}{2} P_{DC} \left(t_d - \frac{1}{2} (\Omega_s - \dot{\Theta}_E)^{-1} \right) + \frac{1}{2} P_{DC} \left(t_d + \frac{1}{2} (\Omega_s - \dot{\Theta}_E)^{-1} \right)$$

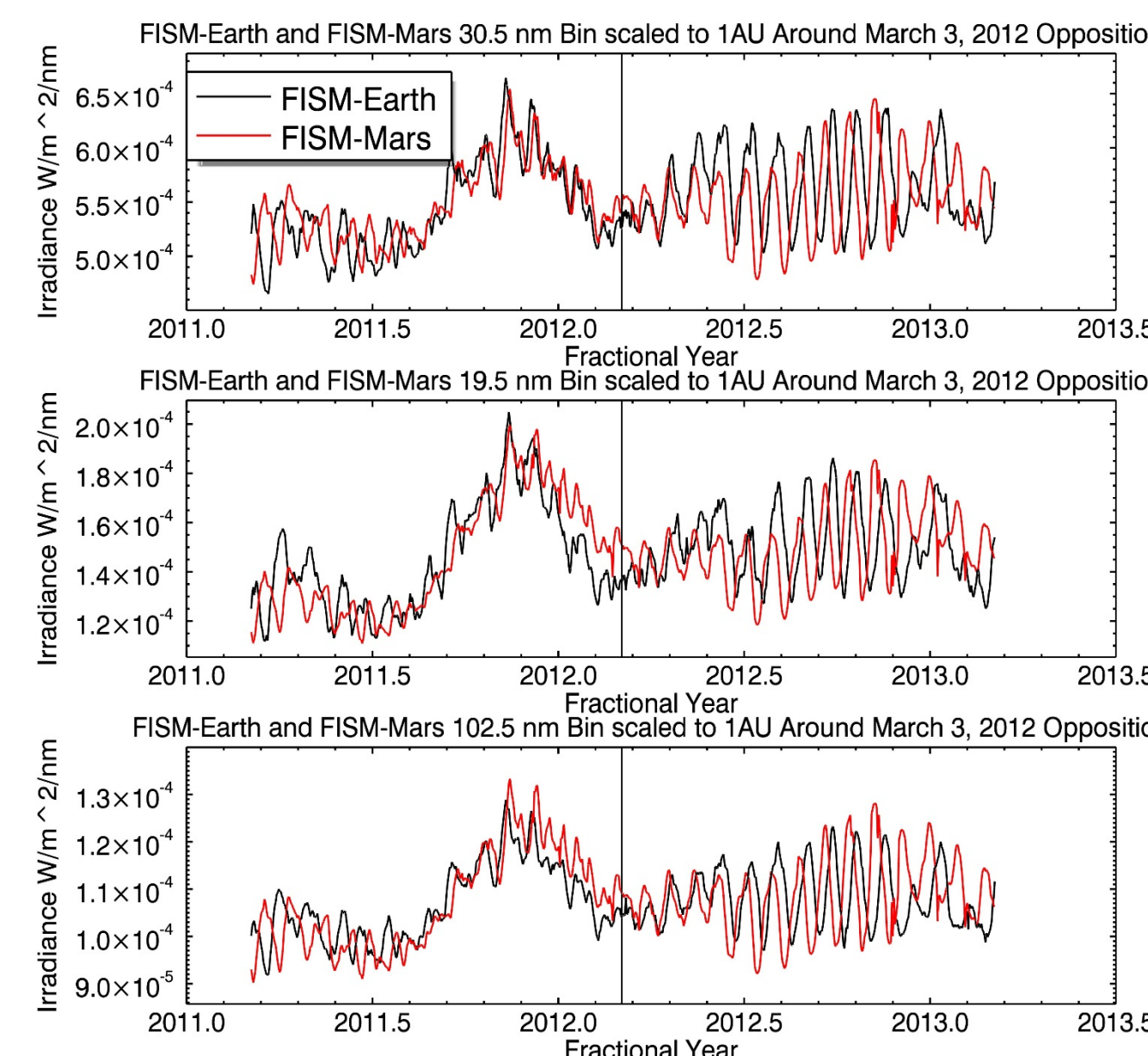
The effectively interpolated training-set proxies represent irradiance at Earth but increasingly suppress features which are transient over a solar rotation for larger CDs.



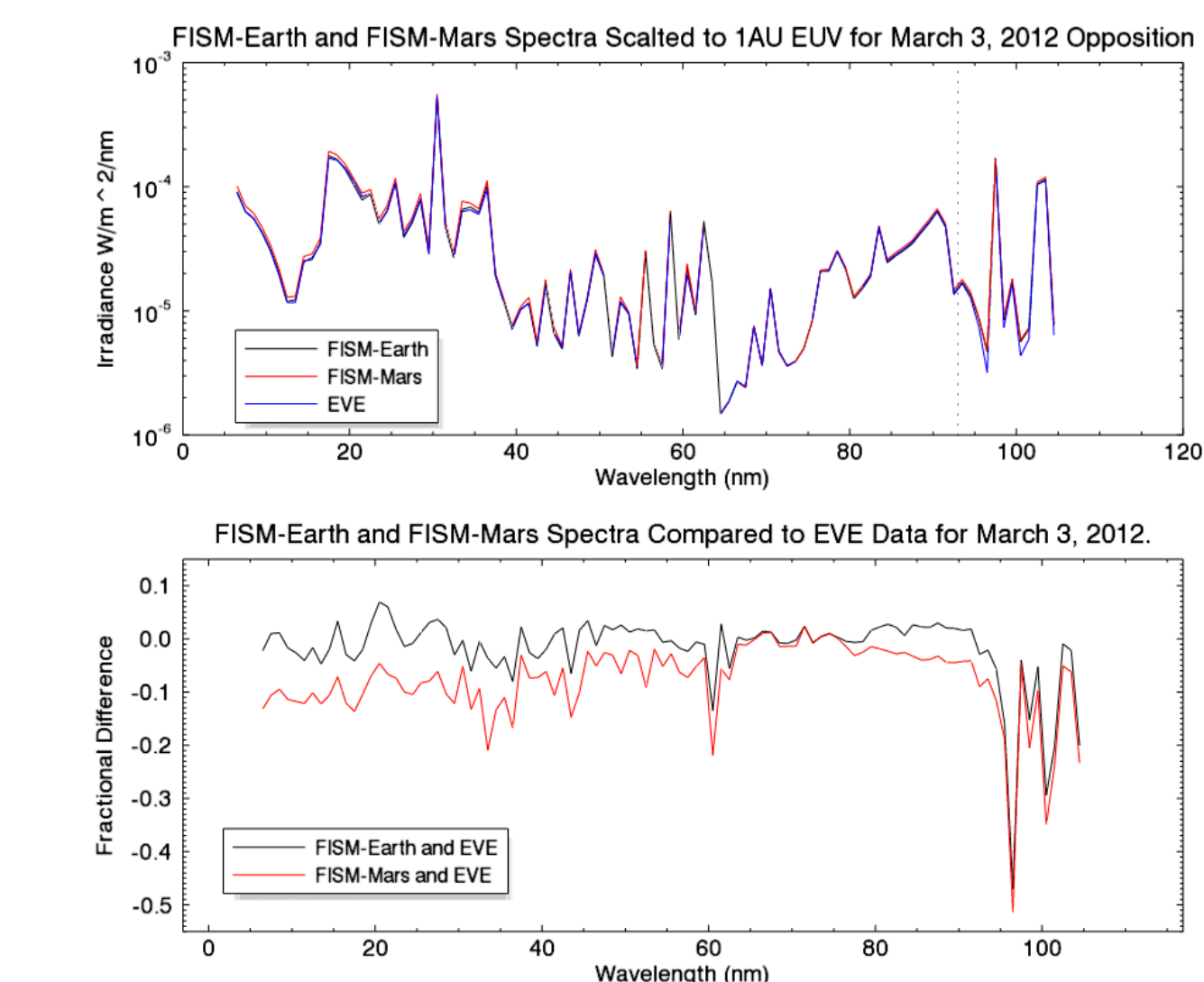
FISM-P interpolates irradiances at Earth around the ecliptic based on Carrington rotation.

RESULTS-DAILY MODEL

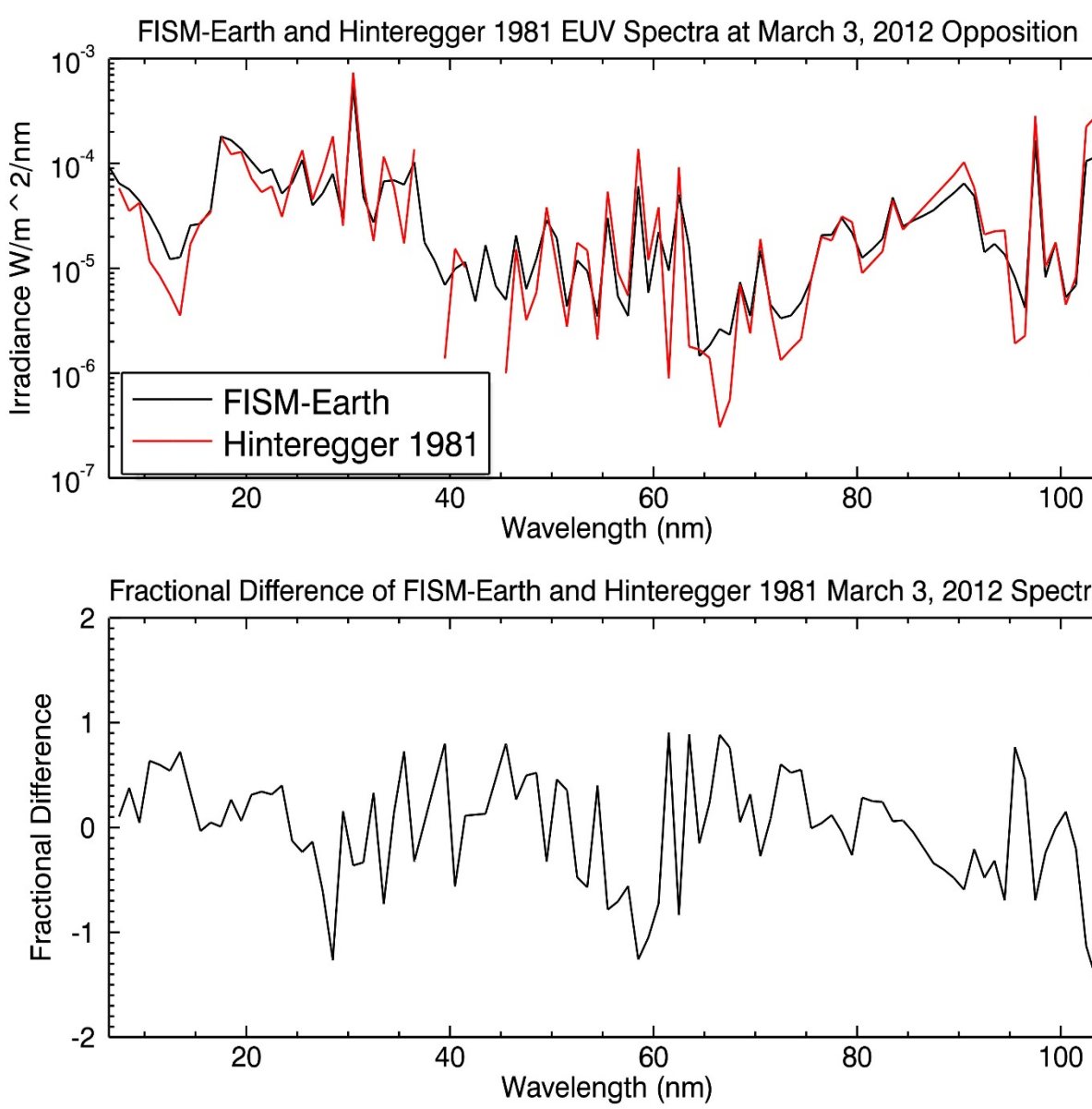
The figures at right compare the FISM-Earth model and the FISM-Mars model. FISM-Earth is configured to use more proxies than FISM-Mars including emissions at 17.1, 30.4, 33.5 and 36.9 nm; whereas the FISM-P data shown for Mars only uses F10.7, H lyman-alpha and Mg II core-to-wing ratio [7,8,9].



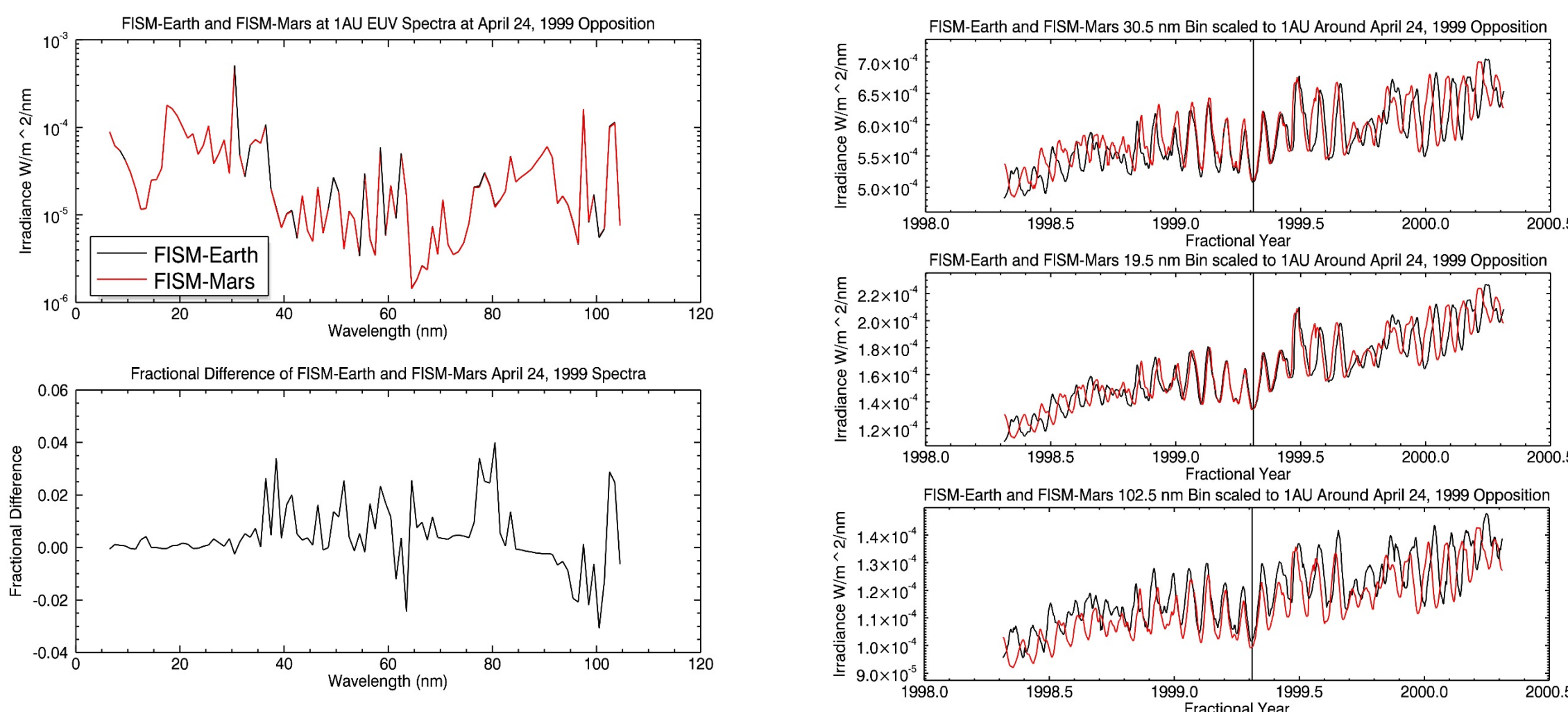
Although FISM-P can also be driven with more proxies to improve accuracy, the model results at right show the performance which can be expected over the relatively large time period (~1978-present) when only F10.7, Lyman-alpha and Mg II c/w are available.



Studies of planetary plasma environments (e.g. [10,11]) often use F10.7 index models such as Hinteregger 1981 to determine the EUV spectral input [12]. The figure at right shows the Hinteregger 1981 model performance for the same date as the FISM-P figures above.



The FISM-Earth and FISM-P results agree well for periods when the same driving proxies are used by both models:



FISM-P performs nearly as well with only 3 common proxies as FISM-Earth does with full suite of 12 proxies.

RESULTS-FLARE MODEL

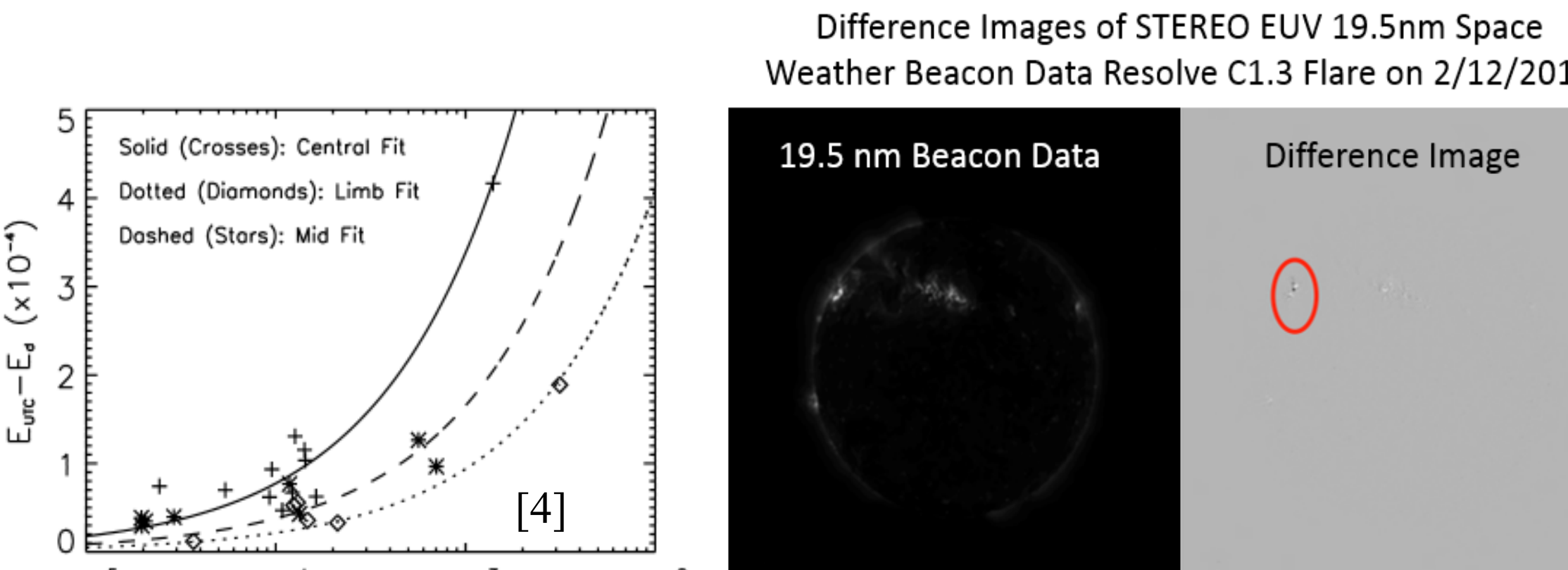
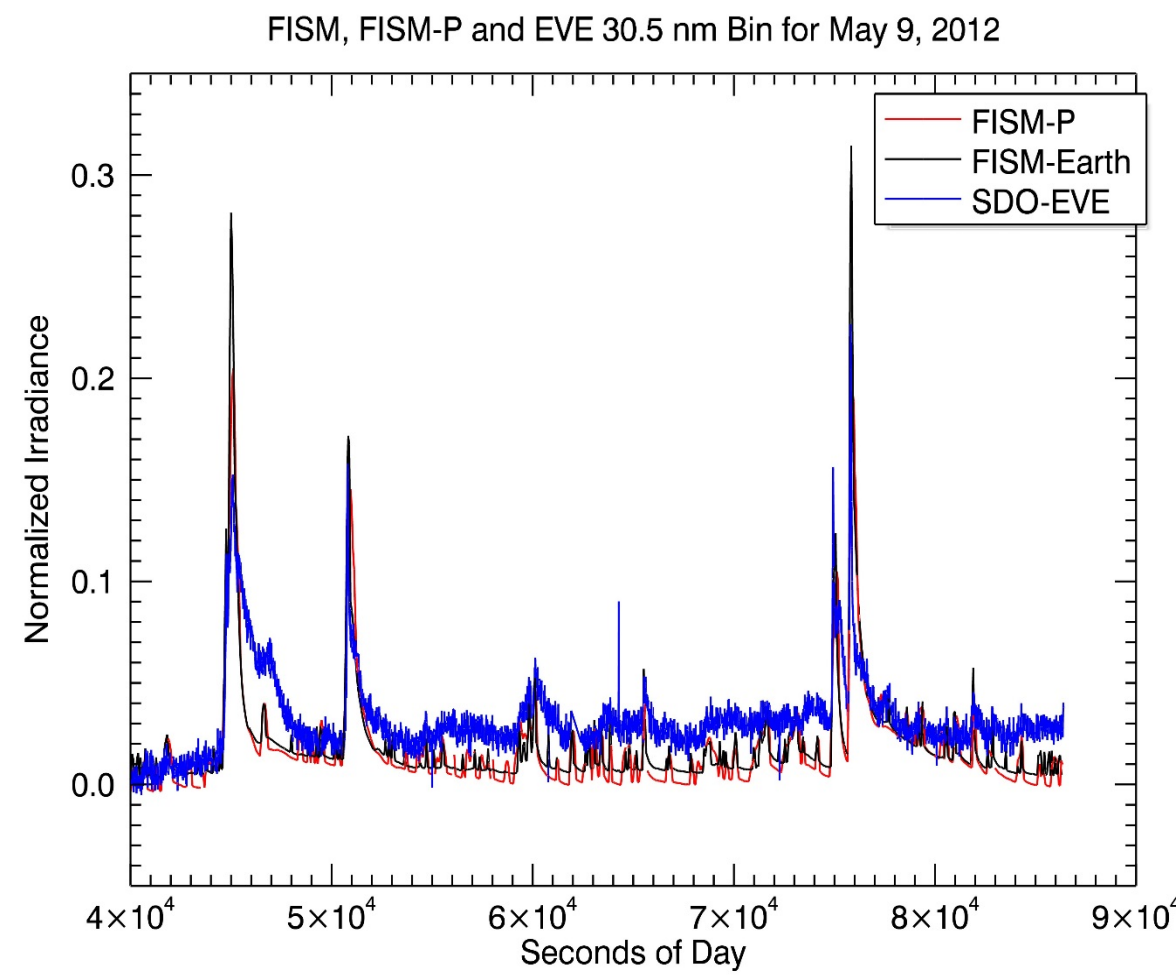
FISM historically models the flare irradiance using the GOES XRS-B, 1 to 8 Angstrom, channel by representing the gradual phase as being proportional to the XRS-B irradiance, and the impulsive phase as being proportional to the derivative of the XRS-B irradiance (Neupert Effect, [13]).

$$E_{flare}(\lambda) = E_{utc} - E_d = \Delta E_{GP} + \Delta E_{IP}$$

$$\Delta E_{GP} = C_{GP} (P_{XRS-B}(t_{UTC}) - P_{XRS-B}(t_d))^{N_{GP}}$$

$$\Delta E_{IP} = C_{IP} \left(\frac{d}{dt} [P_{XRS-B}(t_{UTC}) - P_{XRS-B}(t_d)] \right)^{N_{IP}}$$

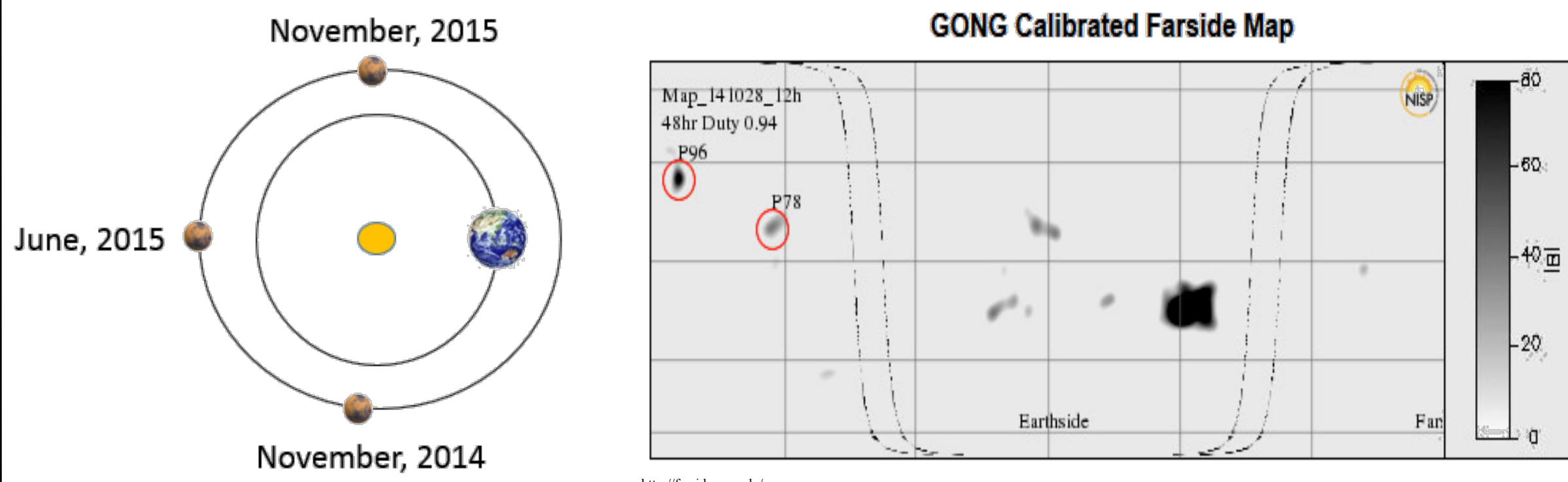
FISM-P has the added capability of modeling flares using the .1-7 nm channels available on SDO-EVE and MAVEN-EUV. See comparison at right. Bins with optically thick emissions such as the 30.5 nm bin shown need a center-to-limb variation correction. Stereo EUVI 19.5 nm Beacon data can resolve flare location if flare is observed by MAVEN-EUV and not Earth.



FISM-P can use 0.1-7 nm flare proxy in lieu of XRS-B to model flares from Mars's vantage point.

MODEL VALIDATION AND IMPROVEMENT

MAVEN will orbit the far-side of the sun during its primary mission from November 2014-November 2015, providing a unique opportunity to validate and improve the daily model interpolation methods. The F10.7 proxy has already been successfully calibrated against earthside magnetograms [14], and a calibration of farside estimated magnetograms from GONG and/or HMI will be attempted. If successful, magnetogram data can be incorporated into the daily model interpolation algorithm, improving accuracy.



FISM-P can possibly use far-side magnetograms as a proxy. MAVEN-EUV can test this concept.

References

- [1] Chamberlin, P.C., T.N. Woods, and F.G. Eparvier. Flare Irradiance Spectral Model (FISM): Daily component algorithms and results. *Space Weather*, 5, S07005, (2007).
- [2] Chamberlin, P.C., T.N. Woods, and F.G. Eparvier. Flare Irradiance Spectral Model (FISM): Flare component algorithms and results. *Space Weather*, 6, S05001, (2008).
- [3] Qian, L., A.G. Burns, P.C. Chamberlin, S.C. Solomon. Variability of thermosphere and ionosphere responses to solar flares. *J. Geophys. Res.*, 116, A10309, (2011).
- [4] Sternovsky, Z., P. Chamberlin, M. Horanyi, S. Robertson and X. Wang. Variability of the lunar photoelectron sheath and dust mobility due to solar activity. *J. Geophys. Res.*, 113, A10104, (2008).
- [5] Lollo, A., P. Withers, K. Fallows, Z. Girazian, M. Matta and P.C. Chamberlin. Numerical Simulations of the ionosphere of Mars during a solar flare. *J. Geophys. Res.*, 117, A05314, (2012).
- [7] Tapping, K.F. Recent solar radio astronomy at centimeter wavelengths: The temporal variability of the 10.7-cm flux. *J. Geophys. Res.*, 92, 829, (1987).
- [8] Vireck, R.A., L.C. Puga, D. McMullin, D. Judge, M. Webster, and W.K. Tobiska. The Mg II index: A proxy for solar EUV. *J. Geophys. Res.*, 28, 1343, (2001).
- [9] Tobiska, W.K. and C.A. Barth. A solar EUV flux model. *J. Atmos. Terr. Phys.*, 53, 1005 (1990).
- [10] Haider, S.A., S.P. Seth, E. Kallio, and K.I. Oyama. EUV and Electro-Proton-Hydrogen Atom-Produced Ionosphere on Mars: Comparative Studies of Particle Fluxes and Ion Production Rates Due to Different Processes. *Icarus*, 159, 18, (2002).
- [11] Fox, J.L. and K.E. Yeager. Morphology of the near-terminator Martian ionosphere: A comparison of models and data. *J. Geophys. Res.*, 111, A10309 (2006).
- [12] Hinteregger, H.E., K. Fukui, and B.R. Gilson. Observational, reference, and model data on solar EUV, from measurements on AE-E. *Geophys. Res. Lett.*, 8, 1147, (1981).
- [13] Neupert, W.N. A comparison of solar X-ray line emission with microwave emission during flares. *Ap J.*, 153, L59, (1968).
- [14] Parker, D.G., R.K. Ulrich, J.M. Pap. Modeling solar UV variations using Mount Wilson Observatory Indices. *Solar Physics*, 177, 229 (1998)